

Viscoelastic and Morphological Behavior of Hybrid Styryl-Based Polyhedral Oligomeric Silsesquioxane (POSS) Copolymers

A. ROMO-URIBE,^{1*} P. T. MATHER,² T. S. HADDAD,³ J. D. LICHTENHAN⁴

¹ Systran Corporation, Air Force Research Laboratory, Materials Directorate, AFRL/MLBP Building 654, 2941 P Street, Suite 1, Wright-Patterson Air Force Base, Ohio 45433-7750

² Air Force Research Laboratory, Materials Directorate, AFRL/MLBP Building 654, 2941 P Street, Suite 1, Wright-Patterson AFB, Ohio 45433-7750

³ Raytheon STX Corporation, Air Force Research Laboratory, Propulsion Directorate, AFRL/PRSM, 10 E. Saturn Blvd., Edwards Air Force Base, California 93524-7680

⁴ Air Force Research Laboratory, Propulsion Directorate, AFRL/PRSM, 10 E. Saturn Boulevard, Edwards Air Force Base, California 93524-7680

Received 24 June 1997; revised 29 January 1998; accepted 2 February 1998

ABSTRACT: We report on the viscoelastic behavior of linear thermoplastic nonpolar hybrid inorganic-organic polymers. These materials have been synthesized through copolymerization of an oligomeric inorganic macromer with 4-methylstyrene where the inorganic portion of the material is a well-defined polyhedral oligosilsesquioxane (POSS), $R_7(\text{Si}_8\text{O}_{12})(\text{CH}_2\text{CH}_2\text{C}_6\text{H}_4\text{CH}=\text{CH}_2)$, with $R = \text{c-C}_6\text{H}_{11}$ or $\text{c-C}_5\text{H}_9$. A series of 4-methyl styrene copolymers with approximately 4, 8, and 16 mol % POSS macromer incorporation were investigated. Rheological measurements show that the polymer dynamics are profoundly affected as the percent of POSS increases. In particular, a high-temperature rubbery plateau develops (where a terminal zone is not observed), despite the fact that the parent poly 4-methylstyrene is unentangled. It is also observed that the thermal properties are influenced as the percent of POSS incorporation increases, with increases in the glass and decomposition temperatures. The results suggest that interchain interactions between the massive inorganic groups are responsible for the retardation of polymer chain motion, a mechanism similar to the "sticky reptation" model conceived for hydrogen-bonded elastomers and developed by Leibler et al. [*Macromolecules*, **24**, 4701 (1991)]. Control over the interchain interactions would also give rise to the observed increases in glass transition and the establishment of a rubbery plateau. © 1998 John Wiley & Sons, Inc. *J Polym Sci B: Polym Phys* 36: 1857-1872, 1998

Keywords: hybrid polymers; rheology; reptation; silsesquioxane polymers

INTRODUCTION

The recent development of several families of hybrid reagents and polymerizable macromers

based on polyhedral oligomeric silsesquioxanes (POSS) affords a tremendous opportunity for the preparation of new thermoset and thermoplastic material formulations.¹⁻⁴ As part of our ongoing effort to investigate, understand, and develop these materials as new classes of plastics for aerospace applications we have now initiated investigation into their rheological and mechanical properties.

* Present address: Hoechst Research and Technology, 86 Morris Ave., Summit, NJ 07901

Correspondence to: P. T. Mather

Journal of Polymer Science: Part B: Polymer Physics, Vol. 36, 1857-1872 (1998)
© 1998 John Wiley & Sons, Inc. CCC 0887-6266/98/111857-16

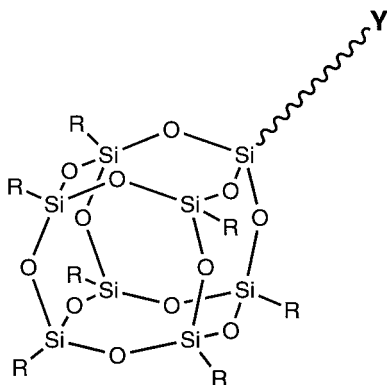


Figure 1. A representative POSS macromer with seven solubilizing R groups and a single Y group for incorporation into a polymer. Such a POSS macromer is used to make a hybrid polymer with a pendant architecture.

As polymerizable reagents, POSS systems are unique in two primary aspects. Their composition is truly hybrid (inorganic–organic), containing an inorganic framework made up of silicon and oxygen ($\text{SiO}_{1.5}$), which is externally covered (and solubilized) by hydrocarbon substituents. The physical size of POSS reagents is unique in that it is macromeric with respect to most polymer dimensions. The typical POSS macromer containing cyclohexyl groups approaches a molecular weight of 1000 amu and is approximately 14 Å in diameter.⁵ These two features and the fact that such systems are readily copolymerized with most wholly organic mers provides the materials chemist with a new means of introducing and manipulating many properties of established polymer systems (Fig. 1).

It is expected—and has been almost uniformly observed⁶—that the introduction of POSS moieties into the backbone of polymeric chains affects the physical properties of the polymer dramatically. Past studies have revealed a strong dependence of the softening point of these polymers on the level of copolymerization of POSS into such parent polymers as polystyrene, poly(methylmethacrylate), polynorbornene, polyamides, and poly(dimethyl siloxane). Because of the absence of polar units in POSS mers, it is currently hypothesized that the mechanism by which the softening temperature (glass transition) is increased through POSS incorporation is by retardation over large length scales (polymer dimensions) of the polymer chain motion, either via intermolecular interactions or associations between POSS units, or by the large inertia exhibited by a poly-

mer segment containing the massive POSS mers. Consider, for example, the case of styryl-based POSS polymers, the subject of this study, where the linear density, λ , will be approximately 450 amu/Å, whereas for polystyrene the linear density is approximately 60 amu/Å,⁷ a difference of approximately one order of magnitude.

The dynamics of polymers in the condensed state remains at the focus of current debate. Despite the large number of experimental^{8–11} and theoretical^{12–15} results available, the dynamics of such systems is not entirely understood. The reason for this seems to be associated with the local and global dynamics of polymeric chains. The problem of local motion of molecular segments in a condensed system, in which each chain is closely surrounded by other chains, is that there is no free space accessible to a chain segment unless the surrounding segments (which may belong to the same or other chains) move away from its closest neighborhood. On the global scale, the main difficulty consists in the correct consideration of topological constraints imposed on chains moving among other chains under the condition of noncrossability. The reptation or tube model^{12,13} has provided us with the framework for understanding of transport properties in entangled linear polymers; however, the results achieved are not completely satisfactory. The tube renewal process or tube length fluctuations^{14,15} are just two of many examples of modifications to the reptation theory, and are part of an effort to improve our understanding of condensed polymeric systems. Recent developments in polymer chemistry enables controlled synthesis of more complex polymeric architectures where the dynamics of cyclic,¹⁶ star-,¹⁷ or comb-like¹⁸ molecules can now be studied for well-defined systems. Investigations in this field have shown that the properties of such systems cannot be understood within the framework of existing models.¹⁹ In particular, for complex polymeric architectures, POSS copolymers being another example, it would appear that molecular interactions (physical and/or chemical) will play a significant role in the chain dynamics. Indeed, it is not expected that the friction factor parameter appearing in the Doi–Edwards model¹³ will capture all of the effects of interchain interactions.

The rheological properties of thermoplastic polymers containing associating comonomers via interchain hydrogen bonding have been studied both experimentally^{20–22} and theoretically.^{23–25} The effect of hydrogen bonding on the linear viscoelastic properties is dramatic, and results in the

broadening of the rubbery plateau to lower frequencies, a reflection of a broadening of the relaxation time spectrum in the material. Theoretically,²⁵ it is predicted that the presence of potential association sites along polymer chains in an entangled (monodisperse) melt will lead to a distinct linear viscoelastic response featuring a long relaxation time related to the association lifetime and a secondary rubbery plateau scaling inversely in magnitude with the distance between active association sites. In this description, therefore, associations can act much the way entanglements do, by effectively decreasing the entanglement molecular weight in an already entangled melt, or adding effective entanglements to a melt below the critical molecular weight for entanglement coupling.

This article reports the rheological characterization for a series of nonpolar copolymers of styryl-based POSS macromers and 4-methylstyrene, with special emphasis given to the effect of the pendent POSS group. In this study two types of POSS–styryl macromers were utilized, those with R = cyclopentyl (CpPOSS) and cyclohexyl (CyPOSS) groups. Copolymerization was varied from 4 to 16 mol % POSS. For comparison purposes, we also investigated the rheological properties of the parent homopolymer of 4-methylstyrene. It is important to observe that our study has focused on relatively high POSS weight fractions. For example, the relatively low concentration of 8 mol % POSS comonomer corresponds to approximately 50 wt % POSS in the resulting material. Our results will show that POSS incorporation substantially modifies the thermal and rheological properties of the polystyrene where above a certain “critical” mol % content, characteristic of each type of POSS mer, the interchain and/or intrachain POSS interactions gives rise to a rubbery plateau in otherwise unentangled polymers.

EXPERIMENTAL

Polymer Synthesis

The preparation of POSS macromers has been described in detail elsewhere.^{2–4} They have a roughly spherical (Si_8O_{12}) inorganic core, surrounded by seven inert alkyl groups for solubility and, in the case of the styryl derivative, one reactive ethylstyrene group for polymerization (Fig.

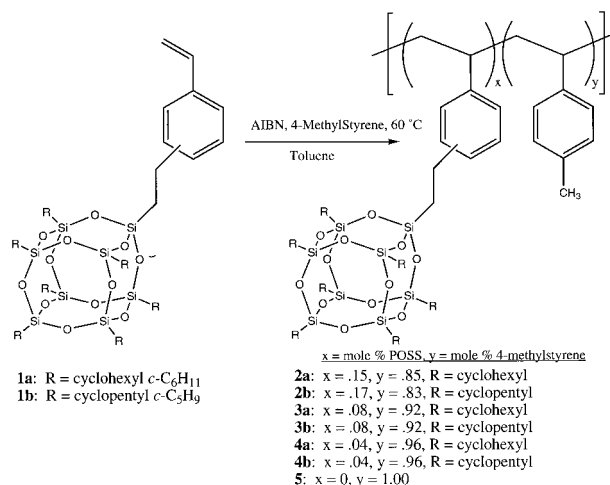


Figure 2. POSS styryl macromer copolymerization.

2). The copolymers and poly(4-methylstyrene) were all synthesized by free radical polymerization under nitrogen atmosphere using AIBN as initiator, and a reaction time of 64 h at 60°C (Fig. 2). The structure in the polymers was confirmed via ^1H and ^{29}Si nuclear magnetic resonance (NMR).^{3,4} Using NMR, it was observed that the composition of POSS comonomer in the polymers was insensitive to the total extent of monomer conversion, indicating similar reactivity of the monomers and minimizing the possibility of comonomer segregation along the chain. Average molecular weights and molecular weight distributions were determined by gel permeation chromatography (GPC) and a combination of refractive index and multiangle laser light scattering measurements with a Wyatt Technologies DAWN spectrometer. Values of \bar{M}_w and the ratio \bar{M}_w/\bar{M}_n are listed in Table I. We note that \bar{M}_w for poly(4-methylstyrene) is lower than the critical molecular weight for entanglements, $M_c \sim 38,000 \text{ g/mol}$, where $M_c = 2M_e$, and M_e is the molecular weight between entanglements.¹¹

Thermal Analysis

The thermal analysis was conducted using a DuPont 2000 Thermal Analyzer, and the thermogravimetric analysis (TGA) was carried out on a DuPont TGA 951 under nitrogen atmosphere; the heating rates utilized were 10°C/min. Glass transitions were determined using a DuPont TMA 2940 thermomechanical analyzer (TMA) under nitrogen atmosphere and with a heating rate of 3°C/min and a mechanical force of 0.1 N. Addi-

Table I. Molecular Properties of Styryl-Based Hybrid Copolymers and Parent Homopolymer

Compound	R	mol % POSS ^a	wt % POSS	$M_w \cdot 10^3$ (g/mol)	M_w/M_n	DP	T_g (°C) ^b	T_{dec} (°C) ^c
2a	Cp	15	63	109	1.49	270	146	410
2b	Cy	17	64	60	1.43	154	109, 205	407
3a	Cp	8	45	102	1.42	363	136	402
3b	Cy	8	42	120	1.52	419	122	399
4a	Cp	4	28	85	1.57	343	131	378
4b	Cy	4	27	61	1.36	291	122	383
5	—	0	0	34	1.62	178	119	388

^a mol % POSS in the polymer determined from ¹H-NMR spectra.

^b T_g determined from the softening point of a pressed pellet on second heating using thermomechanical analysis.

^c T_{dec} reported as the temperature at which 10% weight loss has occurred using thermogravimetric analysis.

tionally, differential scanning calorimetry (DSC) was performed using a Perkin–Elmer DSC-7 to confirm glass transition temperatures measured with TMA and to determine the existence of any melting endotherms. For these tests, samples weighing approximately 10 mg were heated at 10°C/min under a flow of N₂. Listed in Table I are the glass transition temperatures and decomposition temperatures. Figure 3 shows the dependence of these material characteristics on the mol percentage of POSS comonomer for both CyPOSS and CpPOSS.

X-ray Scattering

To examine potential POSS-derived alteration of solid-state polymer microstructure in the POSS-PS copolymers, X-ray scattering analysis was performed. Wide-angle X-ray scattering (WAXS) patterns of the as-polymerized powders were obtained in symmetrical transmission mode using a Rigaku rotating anode generator with Cu target and graphite monochromator. Patterns were recorded on film using a Statton camera, and d-spacings were calibrated with Si powder standard. Patterns were digitized using a Molecular

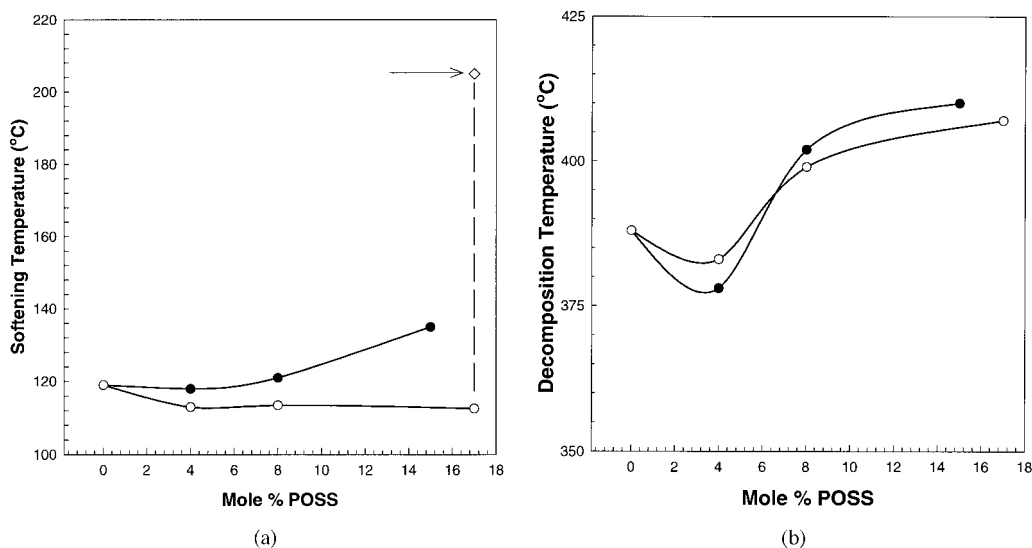


Figure 3. (a) Glass transition temperatures, T_g , as a function of mol % composition of POSS units. T_g s were determined from the softening point of a pressed pellet on a second heating using thermomechanical analysis. (b) Decomposition temperatures, T_{dec} , as a function of mol % composition of POSS units. T_{dec} reported as the temperature at which 10% weight loss has occurred from a powdered sample heated under nitrogen at 10°C/min. Symbols are for CpPOSS, closed symbols are for CyPOSS.

Dynamics microdensitometer for further analysis. Small-angle X-ray scattering experiments were performed at CHESS Synchrotron facilities at Cornell University. Diffraction patterns were obtained in symmetrical transmission mode and recorded on image plates.

Rheological Characterization

The rheological properties of the polymers were measured with a RMS 605 rheometer manufactured by Rheometrics, Inc. It was equipped with 25 mm diameter parallel plates and a 2,000 g·cm torque transducer. The existence and extent of the linear viscoelastic (LVE) regime was determined measuring the dynamic storage and loss moduli, $G'(\omega)$ and $G''(\omega)$, as a function of strain, γ , at 10 rad/s strain rate. The linear viscoelastic properties were measured as a function of strain rate, ω , by subjecting the sample to small sinusoidal strains (1–10%). Measurements were performed under nitrogen atmosphere and at temperatures from 160 to 340°C, the exact range depending of the POSS content in the polymers. The temperature control was better than $\pm 0.5^\circ\text{C}$. The frequency range was sufficiently large so that in most cases data were obtained from the high-frequency transition region down to the low-frequency terminal region. In addition, the relaxation modulus [$G(t)$] was measured by examining the material response to a step shear strain using a Rheometrics RDA-II rheometer with parallel plates. The step strain magnitude used in these experiments was 20%.

The experimental protocol was as follows: the rheometer was heated to the desired temperature, allowed to equilibrate and the gap separation set. As-polymerized fresh samples were loaded in the preheated rheometer, heated at 30°C/min, and holding for 10 min to allow for thermal and deformation equilibrium before measurements started. Experiments were repeated to check reproducibility, and in each case a fresh sample was used. Thermal cycles were also performed to investigate possible effects of thermal history. The stability of the polymers, after rheological measurements, was monitored using NMR spectroscopy and GPC.

RESULTS

Morphology

Figures 4 and 5 show the wide-angle X-ray scattering patterns corresponding to the CpPOSS and

CyPOSS copolymers, respectively. In comparison with the poly(4-methyl styrene), where only one amorphous halo is observed at about $19^\circ 2\theta$, we can see that the 4 mol % CpPOSS copolymer exhibits two diffuse halos, Figure 4(a), where the position of the amorphous maxima are approximately $8.6^\circ 2\theta$ and $18.7^\circ 2\theta$. The observed 10.3 Å length scale is smaller than the maximum diameter of the POSS groups (~ 14 Å), indicating that some interpenetration of the corner groups occurs during packing. As the CpPOSS comonomer fraction increases, the intensity of the $8.6^\circ 2\theta$ peak increases drastically, Figure 4(b), while the 2θ width decreases. At 17 mol % CpPOSS, this peak shifts to $\sim 8.4^\circ 2\theta$ and further sharpens to a well-defined crystalline peak. On the other hand, the amorphous halo at $18.7^\circ 2\theta$ increases in intensity (i.e., the 2θ width decreases) [Fig. 4(b)], and gradually shifts to a larger angle ($\sim 19.1^\circ 2\theta$) at 17 mol % CpPOSS [Fig. 4(c)]. In Figure 4(c) it is also seen that a crystalline ring has formed superimposed on the outer amorphous halo. These features are better appreciated in the corresponding 2θ intensity traces shown in Figure 4(d). The shifting of the X-ray peaks as the CpPOSS content increases is associated with an expected transformation of the crystallographic structure of the copolymers (as CpPOSS content increases) to that of the CpPOSS homopolymer, as has been observed in other systems.^{26,27} The CpPOSS homopolymer is semicrystalline and displays a sharp peak at $8.4^\circ 2\theta$ (10.21 Å), a slightly weaker and broader peak at $19.1^\circ 2\theta$ (4.57 Å), a broad peak at $24.7^\circ 2\theta$ (3.54 Å), and a weak broad peak at about $39.5^\circ 2\theta$ (2.2 Å). The positions of the first three peaks are indicated with vertical dashed lines in Figure 4(d). From the width of the crystalline peak at $8.4^\circ 2\theta$, it has been possible to estimate the crystallite size in the 17 mol % CpPOSS copolymer using the Scherrer formula.²⁸ For this we are assuming that paracrystalline distortions that are known to broaden crystalline peaks are negligible,²⁹ which may not be the case. Nevertheless, our purpose is to obtain an order of magnitude of the crystallite size present in the material. We estimate a crystallite size of ~ 80 Å. In agreement with our morphological characterization we note that the 17 mol % CpPOSS copolymer is the only sample to exhibit a DSC melting endotherm (at 207°C), and, therefore, the rheological characterization described below was carried out above this temperature.

The X-ray patterns corresponding to CyPOSS copolymers present similar features to those de-

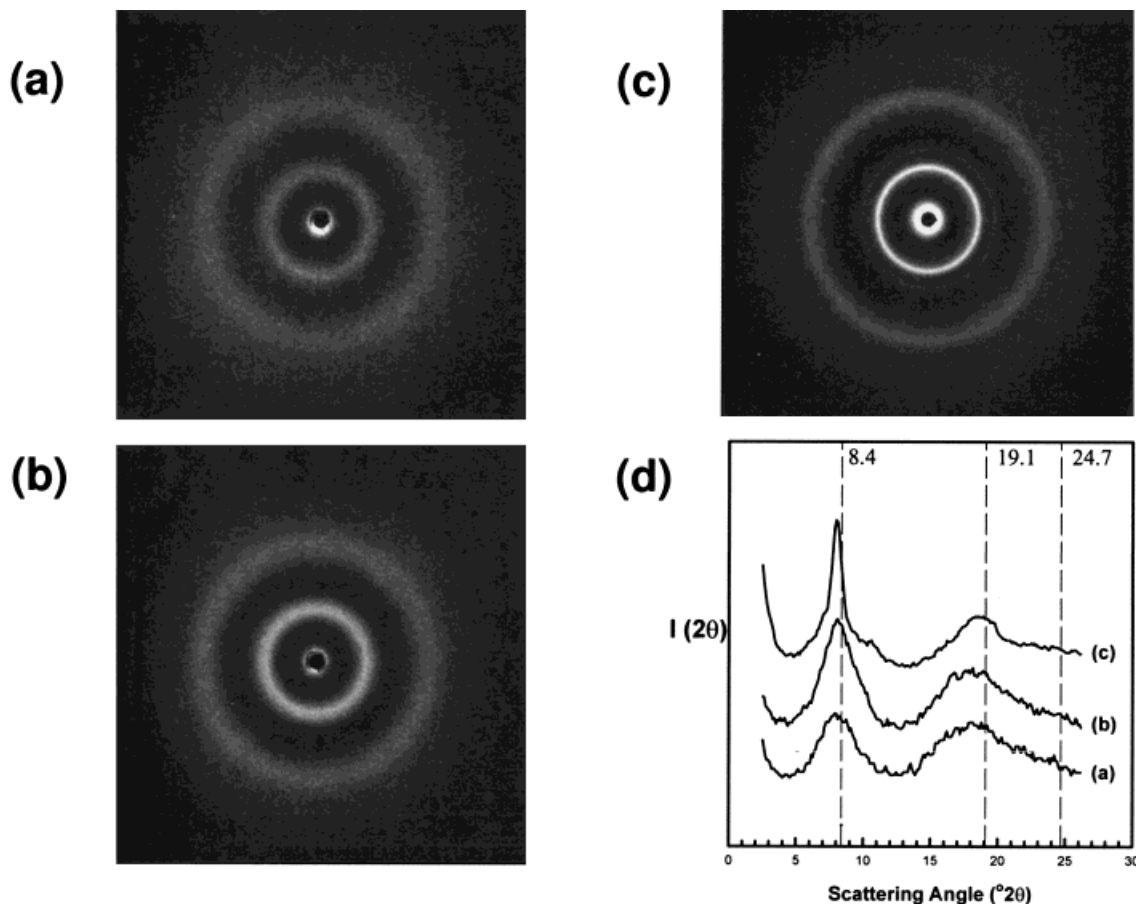


Figure 4. Wide-angle X-ray scattering patterns of as-polymerized CpPOSS copolymers of (a) 4 (**4b**), (b) 8 (**3b**), and (c) 17 (**2b**) mol % POSS content. (d) Optical density as a function of scattering angle 2θ of the patterns shown in (a)–(c) Cu target and graphite monochromator were used.

scribed for their CpPOSS counterparts. However, there are subtle differences that we would like to address. There is a relatively strong peak at $8.4^\circ 2\theta$, even at the lowest CyPOSS concentration. However, it only sharpens slightly with increasing concentration. Comparing the $^\circ 2\theta$ intensity traces for the 17 mol % CpPOSS and 15 mol % CyPOSS copolymers, traces (c) in Figures 4(d) and 5(d), and considering that the same trend is also observed with the respective homopolymers, we suggest that the broadening of the $8.4^\circ 2\theta$ peak is probably associated with crystalline distortions (distortions of the first kind²⁹) introduced by the additional methylene unit in the cyclohexyl group. These distortions prevent better packing in the material, and this is the reason why a melting endotherm is not observed in this case. We note that the outer, rather broad, peak shifts from about $18.4^\circ 2\theta$ (4 mol %) to about $17.8^\circ 2\theta$ (15 mol %) with no appreciable change in the $^\circ 2\theta$ width. As

was previously discussed, the peak shift corresponds to a modification of the microstructure toward that of the CyPOSS homopolymer. The powder diffraction pattern of the CyPOSS homopolymer shows that it is semicrystalline and presents a strong peak at $8.4^\circ 2\theta$ (10.2 Å), a weaker and broader peak at $17.6^\circ 2\theta$ (4.9 Å), and a weak broad peak at $38.8^\circ 2\theta$ (2.3 Å). A complete crystallographic analysis of these polymers is beyond the scope of this work and will be the subject of a future publication.

Linear Viscoelasticity

Investigation of the linear viscoelastic behavior was carried out by applying strain sweeps at constant strain rate (frequency) of 10 rad/s. Figure 6 shows the magnitude of the complex viscosity, $|\eta^*|$, as a function of strain, γ , for the parent

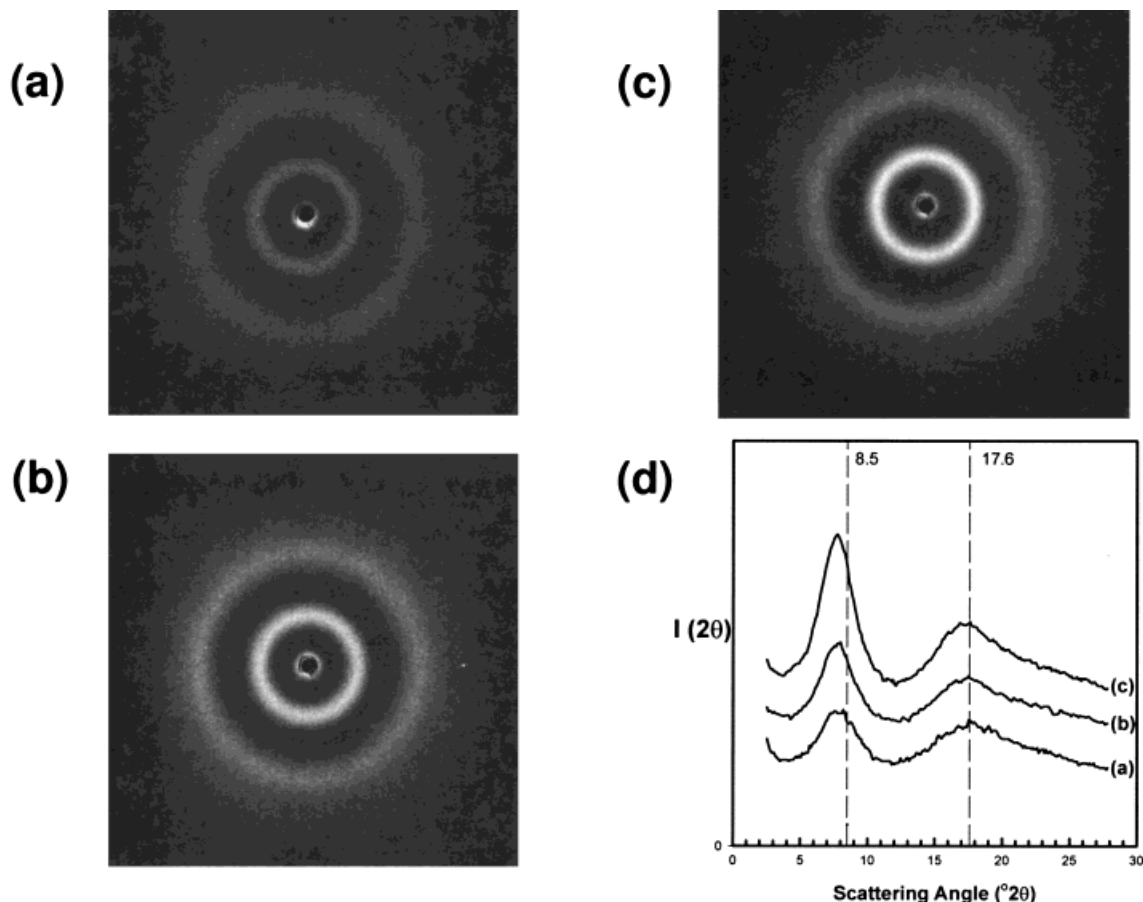


Figure 5. Wide-angle X-ray scattering patterns of as-polymerized CyPOSS copolymers of (a) 4 (**4a**), (b) 8 (**3a**), and (c) 15 (**2a**) mol % POSS content. (d) Optical density as a function of scattering angle 2θ of the patterns shown in (a)–(c). Copper target and graphite monochromator were used.

homopolymer poly(4-methylstyrene) (polymer **5**) and the POSS copolymers. We can see that polymer **5** is linearly viscoelastic (LVE) up to roughly 30% strain. The CpPOSS copolymers are essentially LVE up to about 100% strain for the 4 and 8 mol % compositions (polymers **4b**, **3b**); however, the extent of the LVE regime reduces to about 10% strain for the 17 mol % copolymer (**2b**). Finally, the CyPOSS copolymers (**2a–4a**) are LVE up to 100% strain, independent of their composition.

The dynamic moduli, within the LVE regime were characterized by frequency sweeps performed in a range of temperatures, typically 150 to 240°C for the parent homopolymer and 4 and 8 mol % POSS copolymers, and from 200 to 340°C for the ~16 mol % POSS copolymers.

Time–Temperature Superposition

Logarithmic plots of $G'(\omega)$ and $G''(\omega)$ taken at temperature T were superimposed on those for

temperature T_r by a translation of $\log a_T$ along the frequency axis. No shifts along the modulus axis were required. Time–temperature reduction such as this can be expressed by¹¹

$$G^\#(\omega, T) = G^\#(\omega \cdot a_T, T_r) \quad (1)$$

where the symbol (#) stands for either one prime (') or two primes (''). In this study we chose a reference temperature, T_r , of 180°C.

Figure 7(a)–(d) shows the master curves corresponding to the parent homopolymer, **5**, and the CyPOSS copolymers, while the master curves corresponding to the CpPOSS copolymers are shown in Figure 9(a)–(c). As expected, we see that the parent homopolymer exhibits only the terminal and transition zones, Figure 7(a), confirming that it is unentangled. Interestingly, we find that the polymer **4a**, corresponding to 4 mol % incorporation of the CyPOSS group, also exhibits termi-

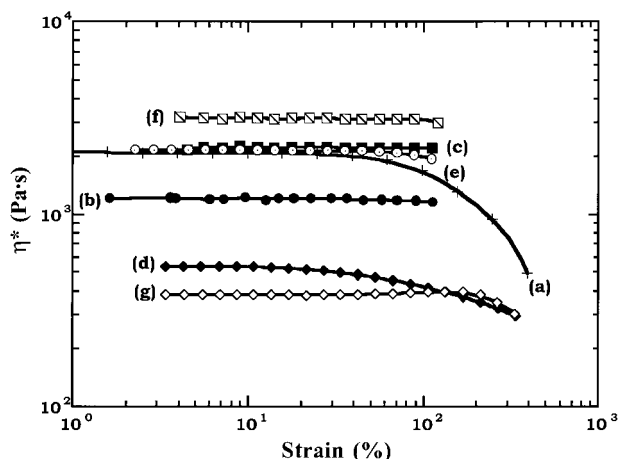


Figure 6. Dynamic viscosity $|\eta^*|$ as a function of strain, γ , for (a) polystyrene (**5**) and (b) 4 (**4b**); (c) 8 (**3b**); (d) 15 (**2b**) mol % CpPOSS copolymers, and (e) 4 (**4a**); (f) 8 (**3a**); and (g) 17 (**2a**) mol % CyPOSS copolymers. Data measured at 10 rad/s and 180°C (a)–(e), 200°C (f) and 300°C (g).

nal and transition zones, as seen in Figure 7(b). In other words, the addition of small amounts of CyPOSS macromer does not significantly affect the rheological behavior observed in the parent homopolymer. It is observed, however, that while the transition zone of the parent homopolymer features a crossing of the storage modulus over the loss modulus (near $\omega \cdot a_T = 20$), the polymer **4a** does not show such a crossing. This may be due to a slight increase in the persistence length afforded by the POSS copolymerization, which would tend to extend the molecular weight regime of Rouse dynamics to higher molecular weights.

Further increase in the mol fraction of CyPOSS groups (polymer **3a**) drastically modifies the rheological response where now we can see the transition zone at high frequencies [$G'(\omega) > G''(\omega)$], a predominantly viscous behavior at intermediate frequencies [$G'(\omega) < G''(\omega)$], and a striking rubber-like behavior at the lowest frequencies investigated, where $G'(\omega)$ overlaps $G''(\omega)$ for a second time [Fig. 7(c)]. We also note that, within the range of temperatures investigated and under the current experimental conditions, it was not possible to attain a terminal regime for this polymer without having significant thermal degradation. As stated before, after rheological testing the samples were redissolved and the chemical structure and molecular weights were confirmed to be intact by using NMR and GPC. In other words, the effect observed in our nonpolar system is reversible.

To see if stress would relax at long times in

sample **3a** (8 mol % CyPOSS), a stress relaxation experiment was performed by applying a step shear strain of magnitude $\gamma_o = 0.2$ to a sample at $T = 240^\circ\text{C}$ and monitoring the resulting shear stress, τ_{xy} , over time. The resulting plot of the relaxation modulus, $G(t) = \tau_{xy}/\gamma_o$, is shown in Figure 8. Consistent with the observed value of the plateau modulus in Figure 7(c), the relaxation modulus, $G(t)$, displays a plateau value of approximately 1000 Pa. Additionally, it is observed that the stress begins to relax after a characteristic time of approximately 150 s, with a terminal slope of approximately 2, although the data are too noisy at these long times to accurately measure this slope. Because the stress is observed to decay (though after a long time of 200 s) it is clear that the sample is not crosslinked but, rather, behaving in a manner akin to an entangled polymer melt with a long relaxation time.

Following the trend observed in the 8 mol % CyPOSS copolymer we note that, at 15 mol % CyPOSS group content (polymer **2a**), the rheological behavior is now predominantly rubber-like up to the highest temperature investigated, 340°C [Fig. 7(d)], where the breadth in range of time scales of the rubber-like plateau has increased with respect to the 8 mol % CyPOSS copolymer, extending over almost 4 decades in frequency. We also note that the quality of satisfaction of time-temperature superposition (TTS) has decreased somewhat in this case. Physical-chemical characterization after the rheological measurements, however, showed that in this case the polymer had suffered crosslinking reactions presumably associated with the elevated temperatures experienced during the rheological experiments. Problems with crosslinking effects have also been detected in some hydrogen-bonded elastomeric systems.³⁰

The 4 and 8 mol % CpPOSS copolymers (polymers **3b**, **4b**) displayed only the transition and terminal regimes [Fig. 9(a) and (b)], observed in the parent homopolymer and 4 mol % CyPOSS copolymer. However, the 17 mol % CpPOSS copolymer, **2b** [Fig. 9(c)], showed a similar behavior to that displayed by the 8 mol % CyPOSS copolymer, **2a**, where a rubber-like behavior was found at the lowest frequencies (highest temperatures) investigated. The physical-chemical characterization after rheological testing showed, however, that crosslinking reactions had also occurred in this system.

Close inspection of the 4 mol % CyPOSS copolymer (**4a**) and 4 mol % CpPOSS (**4b**) counterpart

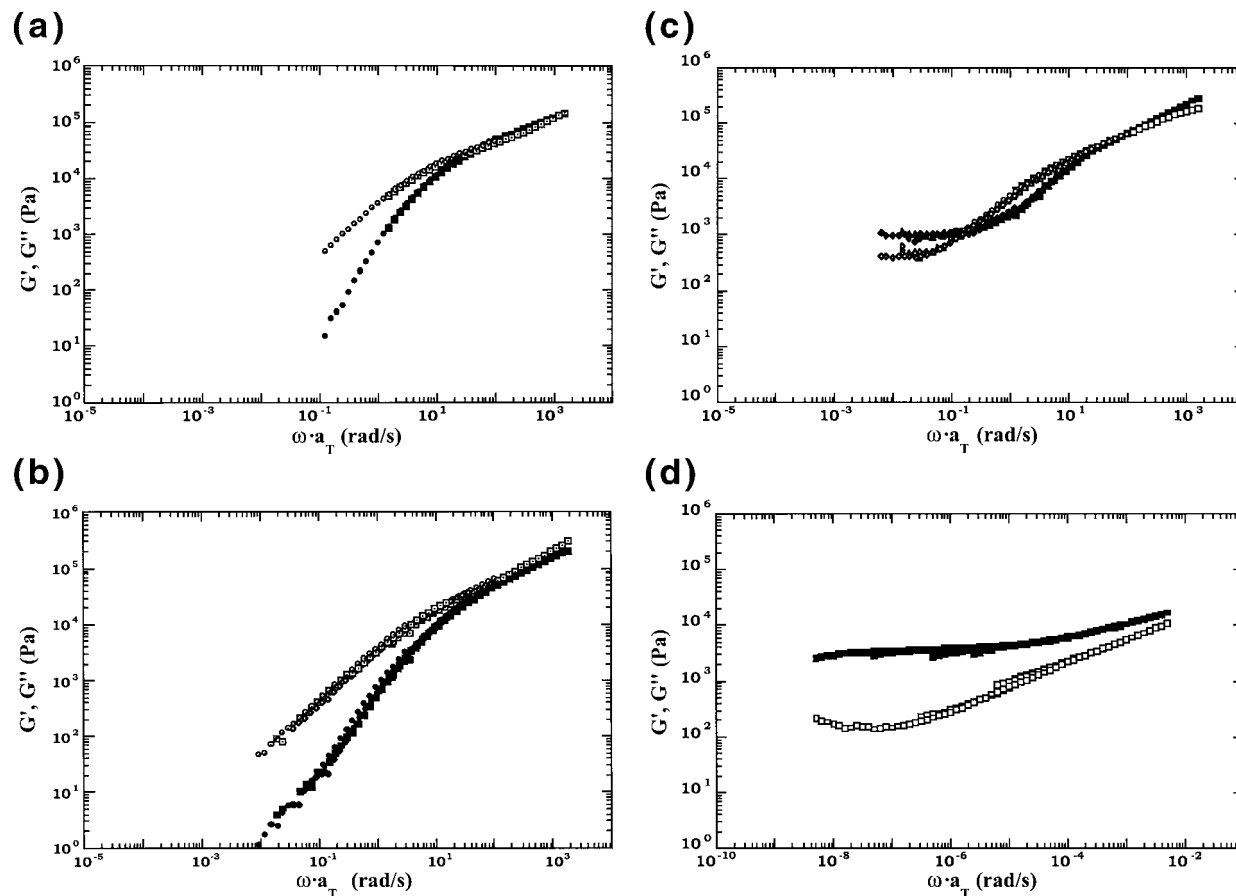


Figure 7. Dynamic moduli $G'(\omega)$ (filled symbols), $G''(\omega)$ (open symbols) master curves for (a) polymethylstyrene (**5**), and (b) 4 (**4a**); (c) 8 (**3a**); and (d) 17 (**2a**) mol % CyPOSS copolymers at a reference temperature of 180°C.

shows that the longest relaxation time of the former is about one order of magnitude larger than that of the latter. Such a strong dependence of the rheological spectra on the nonreactive substituent groups on the POSS mer is surprising, yet consistent with earlier findings on the sensitivity of glass transition to the R group on the cage.⁴

The viscoelastic behavior of the hybrid copolymers is perhaps better appreciated by plotting the mechanical loss angle, $\delta = \tan^{-1}(G''/G')$ [Fig. 10]. We can see that the 4 mol % POSS mers (trace ii) share common features with the parent homopolymer (trace i); however, their δ values are slightly higher, evidencing their predominantly viscous behavior ($\delta \rightarrow 90^\circ$). Trace iii in Figure 10(a) clearly displays the dramatic transition observed in the 8 mol % CyPOSS polymer, varying from predominantly elastic behavior ($\delta \rightarrow 0^\circ$) at low frequencies to predominantly viscous behavior ($\delta \rightarrow 90^\circ$) at intermediate frequencies, and back

to predominantly elastic behavior at high frequencies.

Over the range of temperatures investigated we found that the viscosity follows an Arrhenius form

$$a_T = \eta(T)/\eta(T_r) \propto e^{E_\eta/RT} \quad (2)$$

where T is the absolute temperature, R the ideal gas constant, and E_η is the viscosity activation energy. Typical results are shown in Figure 11, where the shift factors, a_T , for sample **2a** (4 mol % CyPOSS) are plotted using an Arrhenius plot. From the value of the slope, $E_\eta/R = 22,645$ K, we obtain an activation energy of $E_\eta = 188$ kJ/mol. Values of E_η for all of the samples are reported in Table II. It is shown that the values for activation energy range from ~ 190 to 300 kJ/mol. These values are somewhat higher than, but in general agreement with, activation energies measured for

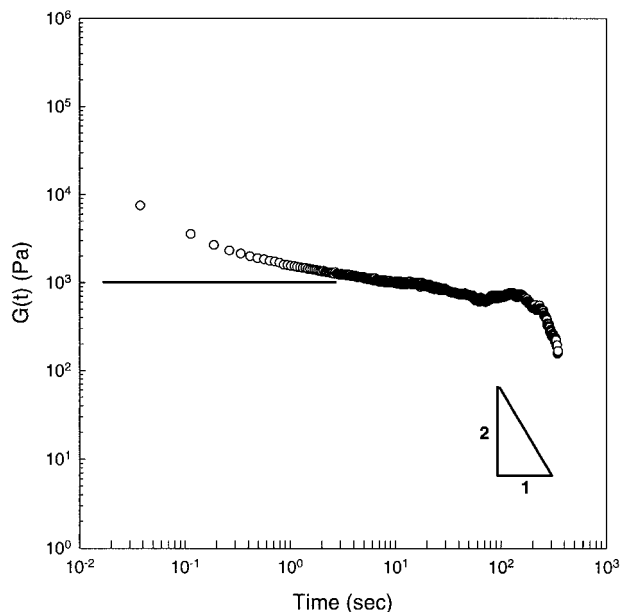


Figure 8. Shear stress relaxation following step shear strain for the 8 mol % CyPOSS copolymer (sample **3a**). The strain amplitude, γ_o , is 0.2 and $T = 240^\circ\text{C}$.

polystyrene (150 kJ/mol),³¹ which is expected to be quite similar to poly(4-methylstyrene).

Behavior in the Terminal Zone

The rheological behavior of the polymeric melts in the long time region, or terminal zone, were characterized by such parameters as the zero-shear viscosity η_o , elasticity coefficient A_G , and steady-state compliance J_e^0 , which are defined respectively as¹¹

$$\eta_o = \lim_{\omega \rightarrow 0} \frac{G''(\omega)}{\omega} \quad (3)$$

$$A_G = \lim_{\omega \rightarrow 0} \frac{G'(\omega)}{\omega^2} \quad (4)$$

$$J_e^0 = \lim_{\omega \rightarrow 0} \frac{G'(\omega)}{G'(\omega)^2 + G''(\omega)^2} = \frac{A_G}{\eta_o^2} \quad (5)$$

with the longest relaxation time, τ , defined as

$$\tau \equiv \eta_o \cdot J_e^0 \quad (6)$$

The results obtained are also listed in Table II.

Effect of Temperature

The influence of temperature on possible morphological changes in these copolymers, such as crys-

tallization, lamellar phase formation, etc., was investigated indirectly by plotting the linear viscoelastic data as $\log G'(\omega)$ vs. $\log G''(\omega)$, a technique that has proven to be useful in the case of linear polymeric chains and block copolymers.^{32,33} Results are shown in Figure 12. We observe that the data for the 4 and 8 mol % POSS copolymers fall on a continuous curve, indicating that no morphological changes occur in the range of temperatures investigated.^{32,33} We also used small-angle X-ray scattering (SAXS) to investigate the possibility of blockiness present in the copolymers. Investigation in a range from 25 to 200 Å on the as-polymerized and heat-treated samples did not provide evidence of long-range order. These results support the view that the rubber-like behavior shown in Figures 7 and 8 is associated with purely physical interactions of the POSS cages.

We also observe that the plots corresponding to the parent homopolymer and 4 mol % copolymers [Fig. 12(a)–(d)], exhibit linear regions that correspond to the terminal zone. The slopes calculated from the linear (terminal zone) regions vary from 1.8 for the parent homopolymer to 1.5 for the POSS copolymers. For linear flexible polymeric materials with molecular weight greater than the molecular weight between entanglements, M_e , and with a single relaxation time, the following analytical expression between $\log G'(\omega)$ and $\log G''(\omega)$ has been derived^{32,33}

$$\log G' = 2 \log G'' - \log(\rho RT/M_e) + \log(\pi^2/8) \quad (7)$$

where ρ is the density, R the universal gas constant, and T the absolute temperature. The temperature-independent behavior observed in Figure 12 can now be understood on the basis of eq. (7). It can be shown that an increase in temperature from T_1 to T_2 will shift the value of $\log G'(\omega)$ by the amount $\log(T_1/T_2)$. Therefore, a change in temperature from 160 to 240°C will shift the value of $\log G'(\omega)$ by the amount 0.17, a negligible variation with respect to the values of $\log G'(\omega)$ and $\log G''(\omega)$. The experimental slope values are slightly lower than that predicted from the Doi–Edwards reptation theory,¹³ a consequence of the polydispersity of the samples.

DISCUSSION

We have shown that a dramatic effect on the thermal and rheological properties of poly-4-methyl

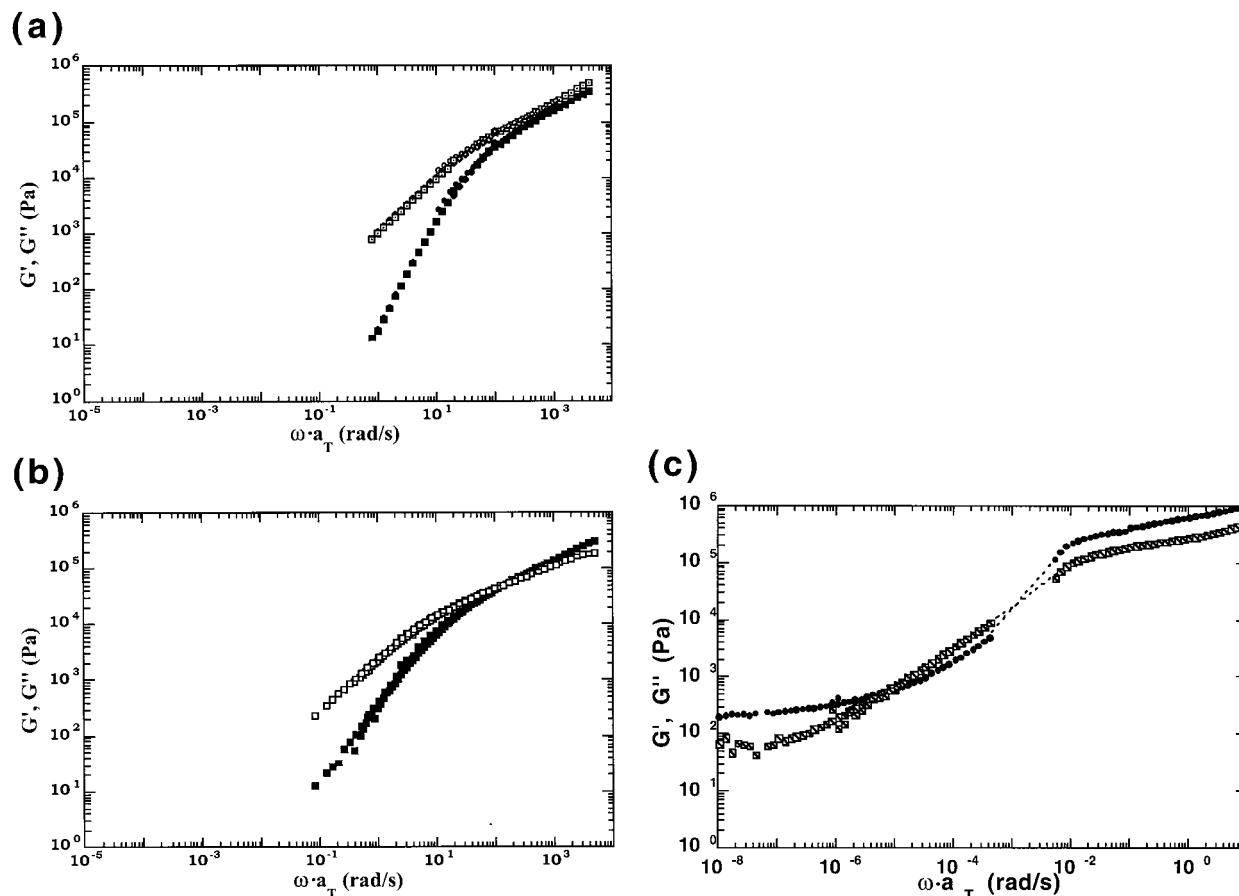


Figure 9. Dynamic moduli $G'(\omega)$ (filled symbols), $G''(\omega)$ (open symbols) master curves for (a) 4 (**4b**); (b) 8 (**3b**); and (c) 16 (**2b**) mol % CpPOSS copolymers at a reference temperature of 180°C.

styrene occurs as a consequence of its copolymerization with POSS macromers, and, in addition, a specific effect of the seven nonreactive POSS substituent groups has also been identified. As was shown in Table I, the molecular weight of the parent homopolymer, **5**, is less than the critical molecular weight for entanglement effects. Therefore, the idea of “sticky reptation” proposed theoretically by Leibler et al. (LRC)²⁵ are not entirely sufficient to explain the underlying mechanism of the surprising rheological modification we have observed. Nevertheless, the LRC model provides an appropriate framework for the discussion of possible polymer dynamics modification mechanisms. Additionally, we would like to propose other possible mechanisms for the modification of the polymer dynamics via POSS incorporation.

Association Effects

In the LRC model it was presupposed that the lifetime of associations between polymer chains is

substantially shorter than the terminal relaxation time of the polymer melt. On the other hand, if it is possible that the lifetime of the associations is longer than the terminal relaxation time, then a secondary plateau (longer times) will feature contributions only from the associations—as the entanglements have all relaxed—and the terminal zone will not be reached except for time scales longer than the association lifetime.

From the data shown in Figure 8 it is apparent that the relaxation time of the associations in these systems is quite large, approximately 150 s. It is worth noting that, under steady shear conditions, a shear thinning effect ought to be observed over a range of shear rates, the product of a yield stress that is a result of the associations present in the polymeric melt. For this reason, it appears that creep or “compression-set” experiments would be quite useful in the examination of these materials.

In explaining the origin of the rubbery modulus

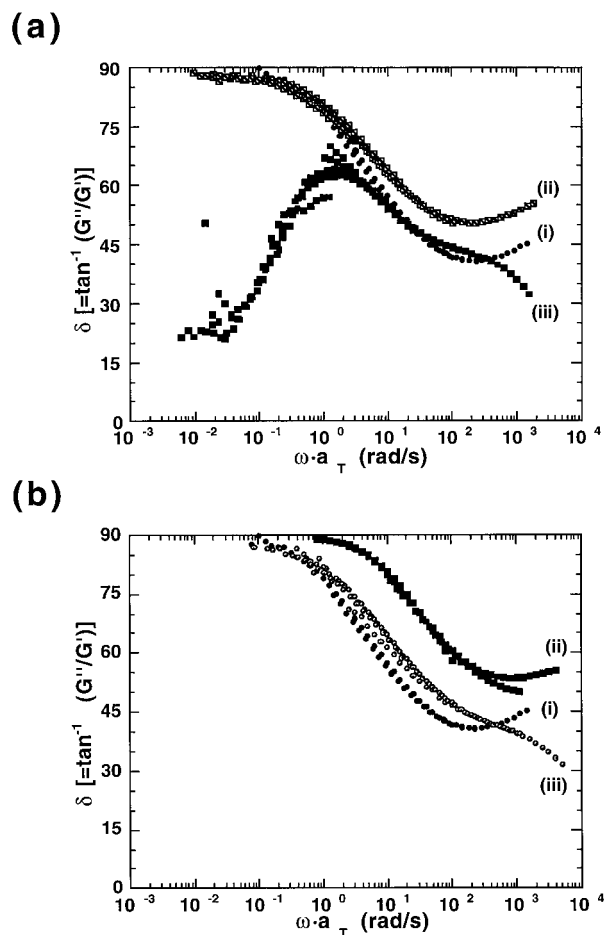


Figure 10. Loss angle, δ , as a function of frequency, ω , at 180°C. (a) Copolymers with (i) 0, (ii) 4, and (iii) 8 mol % CyPOSS content. (b) Copolymers with (i) 0, (ii) 4, and (iii) 8 mol % CpPOSS content.

observed in Figure 7(c) (sample **3a**) we must consider the exceptionally low value of the plateau modulus, ~ 1000 Pa. From rubber elasticity theory³⁴ we know that the plateau modulus can be derived, to first approximation, from the number density of temporary crosslinks (TC) in the material.

$$G_N^0 \approx \nu RT. \quad (8)$$

Here, ν is the number density of TCs, R is the universal gas constant, and T is the absolute temperature. Using eq. (8) with $G_N^0 = 1000$ Pa leads to $\nu \approx 0.25$ mol/m³, which corresponds to a very large linear separation of TCs, λ_{TC} , of 18 nm. For sample **3a**, which possesses 8 mol % CyPOSS monomer, or 50 wt % or vol %, a much larger number density of pairwise associations is possible, ~ 200 mol/m³, corresponding to λ_{TC} of only

2.0–3.0 nm. This order of magnitude difference (2 vs. 20 nm) strongly suggests that, at a given time, only a small percentage of the available POSS comonomers participate in a temporary crosslink, and that clustering of more than two POSS comonomers into each temporary crosslink may occur.

From eq. (8) with $G_N^0 = 1000$ Pa it was surmized that the average distance between temporary crosslinks was approximately 18 nm. Small-angle X-ray scattering measurements of 8% CyPOSS (sample **3a**) under the same conditions as the rheological experiments gave no indication, however, of regular structure on this length scale, as is shown in Figure 13. The peak shown near $S = 0.002 \text{ \AA}^{-1}$ is completely derived from the SAXS beamstop and was present in the absence of the sample. Although this observation suggests that POSS comonomer pairs or clusters are not arranged in a regular array, future experiments are planned using transmission electron microscopy (TEM) to test this conclusion.

The nature of associations between POSS cages is currently under study. Given the absence of polar substituents on the cages, the primary attractive force of interaction between them is likely to be through van der Waals interactions between the cyclohexyl and cyclopentyl substituent groups located in each cage. Although individually each such interaction is very weak, typically between 0.2–0.9 Kcal/mol,³⁵ each POSS cage contains seven substituent groups capable of establishing multiple van der Waals contacts both intra- and intermolecularly. The prospect of multiple interactions could serve to greatly magnify the total associative van der Waals force per cage. Multiple interactions per single structural unit could be a

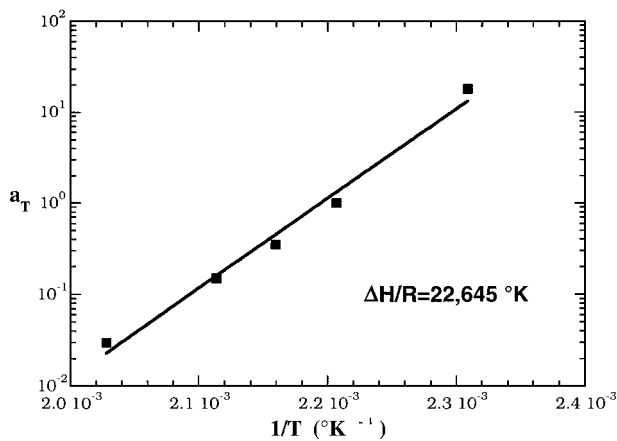


Figure 11. Arrhenius plot of viscosity shift factor, a_T ($=\eta(T)/\eta(T_{\text{ref}})$), for 4 mol % CyPOSS (**2a**).

Table II. Rheological Properties of Stryl-Based Hybrid Copolymers and Parent Homopolymer at 180°C

Compound	η_o (Pa · s)	A_g (Pa · s ²)	G_N° (Pa)	$J_e^\circ \times 10^5$ (Pa ⁻¹)	τ (s)	E_η (kJ/mol)
2a	—	—	4000	—	—	294
2b	—	—	250	—	—	295
3a	—	—	1000	—	150	202
3b	2200	1200	—	24.8	0.54	189
4a	3750	1100	—	8.2	0.31	188
4b	1220	25	—	1.6	0.02	183
5	4000	950	—	6.3	0.25	200

common feature unique to other nanoscale structures as well. Single crystal X-ray diffraction studies as well as computations on POSS monomers support that multiple intermolecular van der Waals interactions between cyclohexyl substituents can indeed occur.³⁶

Inertial Effects

We would like to point to the feasibility to yet another possible mechanism by which POSS moieties can modify rheological properties. Figure 14 shows a schematic diagram in which a POSS moiety has been included into a single polymer chain [Fig. 14(a)], and exists in an entangled state among its neighboring chains. At the instant that a stress is applied to the melt, local segments are deformed, as shown in Figure 14(b). The first mode of relaxation is the reorientation of chain segments via Rouse modes of vibration (short times, high frequency) [Fig. 14(c)], which we feel could be greatly modified in regions near POSS moieties due to inertial effects. As was mentioned in the Introduction, for POSS-PS repeat units the linear density, λ , will be approximately 450 amu/Å, whereas for polystyrene the linear density is approximately 60 amu/Å,⁷ a difference of approximately one order of magnitude. Historically, inertial effects in stress relaxation of polymers have been safely ignored,^{13,37} but it is quite possible that in polymers featuring such a strong contrast in linear density along the polymer chains that such effects may need reexamination.

At later times, further stress relaxation in polymer melts occurs via the mechanism of reptation, or the diffusion of segment density fluctuations along the contour of the polymer backbone, until a time at which any memory of the constraining tube of neighboring chains is gone and stress is completely relaxed. It is likely that this mechanism of stress relaxation is also impacted by the

presence of POSS moieties along the backbone of polymer chains in that the propagation of segment density fluctuations, necessary for the conventional mechanism of reptation, may be significantly attenuated by the large inertial POSS element. This may lead to dramatically altered diffusion of polymer chains in which the usual reptation dynamics are modified to accommodate nondiffusive “anchors,” perhaps more than one per chain. To our knowledge, this is an unexplored area of theoretical polymer dynamics that, with new polymers containing complicated architecture such as the POSS copolymers, or small sized Buckminster fullerene polymers,^{38,39} warrants attention. Large-scale simulations, such as those used by Smith, Hall, and Freeman,⁴⁰ may provide a fruitful approach for such architectures.

Cooperative Dynamics

Rubbery plateaus have been observed in other unentangled polymers that are characterized by such complicated chain architectures as multiarm star polymers (with arms too short to be entangled) or internally crosslinked molecules forming microgels.^{41,42} In these cases, the generally accepted approach of attributing the rubbery plateau to a network of entanglements cannot be supported because of the topological differences among linear chains and multiarm stars and microgels. Pakula et al.⁴³ has shown by utilizing molecular modeling that, in contrast to linear polymers, an ordering process of stars and microgel molecules can be observed. This order causes the translational rearrangements of molecules to begin dominating their dynamics (e.g., the rotational relaxation of star arms is much faster than translational relaxation of the whole molecules). It is possible that a similar effect is active in explaining the rubbery plateau of our unentangled

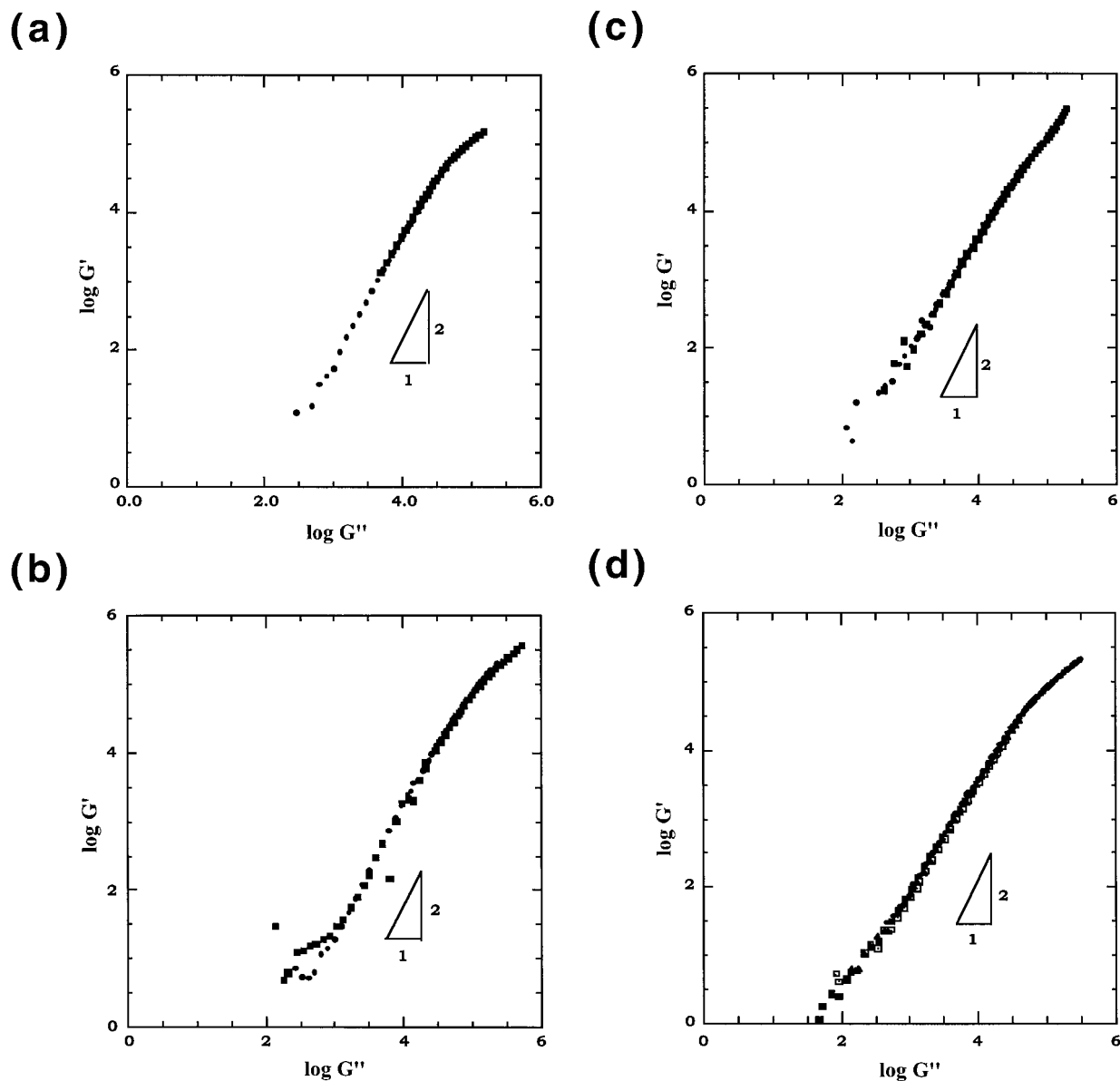


Figure 12. $\log G'(\omega)$ as a function of $\log G''(\omega)$ for (a) polystyrene (**5**), and (b) 4 (**2b**), and (c) 8 (**3b**) mol % CpPOSS copolymers, and (d) 4 (**2a**) and (e) 8 (**3a**) mol % CyPOSS copolymers. The slopes corresponding to the linear (terminal) region in each plot are (a) 1.76; (b) 1.89; (c) 1.57; and (d) 1.50.

POSS-PS copolymer, shown in Figure 7(c). In this scenario, highly cooperative translational rearrangements of POSS macromers need to take place for stress relaxation to occur, in a manner similar to that observed for local rearrangements in dense liquid-like or colloidal systems near a glass transition.⁴¹⁻⁴³ Recall that a POSS content of 8 mol % corresponds to approximately 50% in volume. At such a large volume fraction of roughly spherical objects in a polymer matrix, it is possible

that glass transition-like effects can cause the observed rubbery plateau.

CONCLUSIONS

Thermal and linear viscoelastic properties were determined from a series of styrene-based polyhedral oligomeric silsesquioxane (POSS) macromers copolymerized with 4-methylstyrene by an

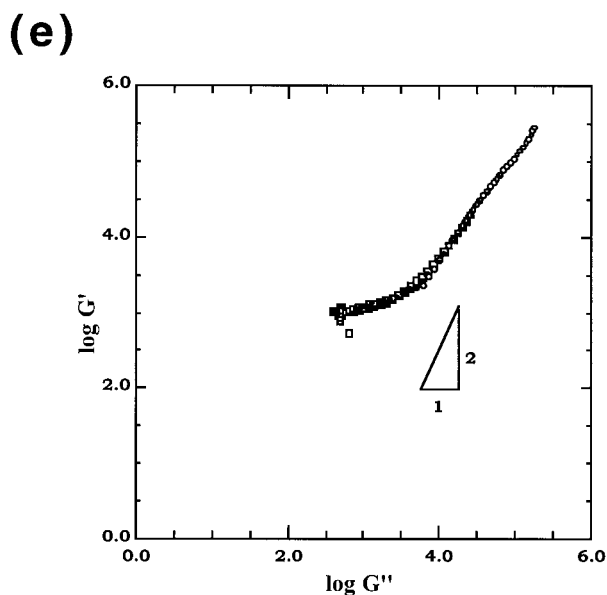


Figure 12. (Continued from the previous page)

AIBN-initiated free radical polymerization. We investigated the effect of the degree of substitution where the concentration of the POSS groups was varied from 0 to 16 mol %. The influence of the pendent POSS group was also investigated by incorporating CpPOSS and CyPOSS macromers. Our results show that the pendent POSS mers modify the thermal properties of the polystyrene supplying greater thermal stability to the parent homopolymer. Furthermore, the rheological char-

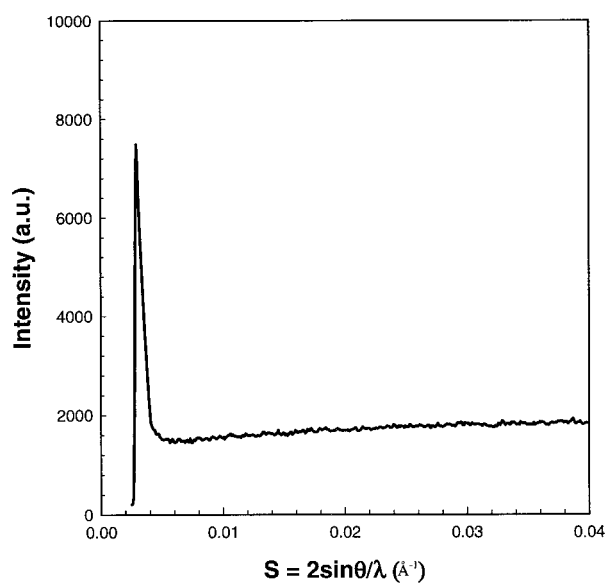


Figure 13. Small angle X-ray scattering (SAXS) of 8 mol % CyPOSS (**3a**) at $T = 240^{\circ}\text{C}$. See text for details.

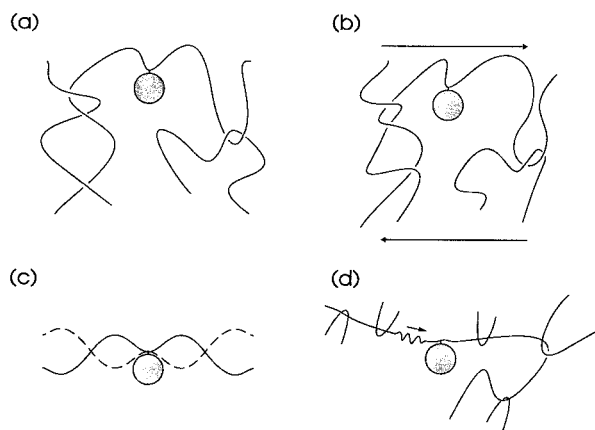


Figure 14. Schematic illustration of potential inertial effects resulting from POSS-incorporation along a polymer backbone. (a) The unstressed state, (b) following an abrupt shearing deformation, (c) Rouse mode modification, and (d) modification of reptation.

acterization showed that, whereas the copolymers with low concentration of POSS mers retain features similar to those of the parent homopolymer, a modification of the polymer dynamics occurs as the concentration of POSS increases, giving rise to a rubber-like behavior at elevated temperatures, where no terminal zone was observed, except in stress relaxation. We suggest that the cooperative translational motion involved in POSS-POSS interactions gives, in some cases, rise to a stable high-temperature elastomeric hybrid material.

This research was supported by the Air Force Office of Scientific Research, Directorate of Chemistry and Life Sciences, and the Phillips Laboratory, Propulsion Directorate. Special thanks to Dr. K. P. Chaffee for providing WAXS data on the styryl-POSS homopolymers, Dr. T. Bunning for performing the SAXS experiments, and to Mr. M. Carr for his help with the molecular weight determination of these polymers.

REFERENCES AND NOTES

1. J. D. Lichtenhan, in *Polymeric Materials Encyclopedia*, J. C. Salamone, Ed., CRC Press, New York, 1996, p. 7768.
2. R. A. Mantz, P. F. Jones, K. P. Chaffee, J. D. Lichtenhan, M. K. Ismail, and M. Burmeister, *Chem. Mater.*, **8**, 1250 (1996).
3. T. S. Haddad, E. Choe, and J. D. Lichtenhan, *MRS Symp. Proc.*, **435**, 25 (1996).
4. T. S. Haddad and J. D. Lichtenhan, *Macromolecules*, **29**, 7302 (1996).
5. The diameter swept out by a $\text{R}_8\text{Si}_8\text{O}_{12}$ POSS mole-

- cule is over 14 Å with an inner Si—Si diameter of 5.4 Å. (a) K. Larsson, *Ark. Kemi*, **16**, 203 (1960). (b) F. J. Feher and T. A. Budzichowski, *J. Organomet. Chem.*, **373**, 153 (1989). (c) T. P. E. Auf der Hyde, H.-B. Burgi, H. Burgy, and K. W. Tornroos, *Chimia*, **45**, 38 (1991).
6. P. T. Mather and J. D. Lichtenhan, unpublished results.
 7. Polystyrene has an average contour length per monomer unit, l_o , of 2.21 Å and a molecular weight per monomer unit, M_o , of 124 amu, giving, therefore, a value of 60 amu/Å for the linear density. In the case of styryl-based POSS polymers, with M_o about 1000 amu, the POSS macromer is pendent to the molecular chain, i.e., it does not form part of the polymer backbone. Therefore, we assume M_o to be approximately 2.21 Å as well, giving a value of 450 amu/Å for the linear density.
 8. T. G. Fox and P. J. Flory, *J. Phys. Colloid Chem.*, **55**, 221 (1951).
 9. W. W. Graessley, *Adv. Polym. Sci.*, **16**, 1 (1974).
 10. R. H. Colby, L. J. Fetters, and W. W. Graessley, *Macromolecules*, **20**, 2226 (1987).
 11. J. D. Ferry, *Viscoelastic Properties of Polymers*, 3rd ed., John Wiley & Sons, New York, 1980.
 12. P. G. DeGennes, *J. Chem. Phys.*, **55**, 572 (1971).
 13. M. Doi and S. F. Edwards, *The Theory of Polymer Dynamics*, Clarendon Press, Oxford, 1986.
 14. W. W. Graessley, *Faraday Symp. Chem. Soc.*, **18**, 7 (1983).
 15. W. W. Graessley, *Adv. Polym. Sci.*, **47**, 67 (1982).
 16. G. B. McKenna, G. Hadziioannou, P. Lutz, G. Held, C. Strazielle, C. Straupe, P. Remp, and A. J. Kovacs, *Macromolecules*, **20**, 489 (1987).
 17. L. J. Fetters, A. D. Kiss, D. S. Pearson, G. F. Quack, and F. J. Vitus, *Macromolecules*, **26**, 647 (1993).
 18. T. F. McCarthy, H. Witteler, T. Pakula, and G. Wegner, *Macromolecules*, **28**, 8350 (1995).
 19. M. Antonietti, T. Pakula, and W. Bremser, *Macromolecules*, **28**, 4227 (1995).
 20. R. Stadler and L. L. Lucca Freitas, *Coll. Polym. Sci.*, **264**, 773 (1986).
 21. L. L. Lucca Freitas and R. Stadler, *Macromolecules*, **20**, 2478 (1987).
 22. M. Muller, U. Seidel, and R. Stadler, *Polymer*, **36**, 3143 (1995).
 23. A. E. Gonzalez, *Polymer*, **25**, 1469 (1984).
 24. L. G. Baxandall, *Macromolecules*, **22**, 1982 (1989).
 25. L. Leibler, M. Rubinstein, and R. H. Colby, *Macromolecules*, **24**, 4701 (1991).
 26. A. H. Windle, *Polymer*, **37**, 2027 (1996).
 27. P. T. Mather and A. Romo-Uribe, *Polym. Eng. Sci.*, to appear.
 28. L. E. Alexander, *X-ray Diffraction Methods in Polymer Science*, R. E. Krieger Pub. Co., New York, 1979.
 29. R. Hosemann and S. N. Bagchi, *Direct Analysis of Diffraction by Matter*, North Holland Pub. Co., Amsterdam, 1962.
 30. C. LeMenestral, P. C. Painter, and M. M. Coleman, unpublished work.
 31. S. Onogi, T. Masuda, and K. Kitagawa, *Macromolecules*, **3**, 109 (1970).
 32. C. D. Han and J. Kim, *J. Polym. Sci., Polym. Phys.*, **25**, 1741 (1987).
 33. C. D. Han and M. S. Jhon, *J. Appl. Polym. Sci.*, **32**, 3809 (1986).
 34. L. H. Sperling, *Introduction to Physical Polymer Science*, John Wiley and Sons, New York, 1986.
 35. Nonbonded attractive intercalations between aliphatic and aromatic systems have been reported by Y. Kodama, K. Nishita, M. Nisho, and N. Nakagawa, *Tetrahedron Lett.*, 2105 (1977); also see J. March, *Advanced Organic Chemistry: Reactions, Mechanisms, and Structure*, McGraw-Hill, New York, 1968.
 36. J. D. Lichtenhan, F. J. Feher, J. W. Ziller, and S. L. Rodgers, unpublished results.
 37. R. G. Larson, *Constitutive Equations in Polymer Melts and Solutions*, Clarendon Press, Oxford, 1988.
 38. C. Weis, C. Friedrich, R. Mülhaupt, and H. Frey, *Macromolecules*, **28**, 403 (1995).
 39. G. D. Wignall, K. A. Affolter, G. J. Bunick, M. O. Hunt, Y. Z., Jr., Menciloglu, J. M. Desimone, and E. T. Samulski, *Macromolecules*, **28**, 6000 (1995).
 40. S. W. Smith, C. K. Hall, and B. D. Freeman, *Phys. Rev. Lett.*, **75**, 1316 (1995).
 41. T. Pakula, S. Geyler, T. Edling, and D. Boese, *Rheol. Acta*, **35**, 631 (1996).
 42. D. Vlassopoulos, T. Pakula, G. Fytas, J. Roovers, K. Karatasos, and N. Hadjichristidis, *Europhys. Lett.*, **39**, 617 (1997).
 43. T. Pakula, *J. Chem. Phys.*, **94**, 2104 (1991).